

## Updated Structural and Conceptual Models For Targeting Temperature Gradient Drilling at the Panyimur Geothermal Prospect, Uganda.

Isa Lugaizi<sup>1</sup>, Nicholas Hinz<sup>2</sup>, William (Bill) Cumming<sup>3</sup>, James Francis Natukunda<sup>1</sup>, Edward  
Mugaddu Isabirye<sup>1</sup>

<sup>1</sup>Directorate of Geological Survey and Mines, Ministry of Energy and Mineral Development  
P.O Box 9 Entebbe.

<sup>2</sup>Nevada Bureau of Mines and Geology, Mackay School of Earth Sciences and Engineering,  
University of Nevada, Reno

<sup>3</sup>Cumming Geosciences 4728 Shade Tree Lane Santa Rosa, CA 95405

[isalugayizi@gmail.com](mailto:isalugayizi@gmail.com), [nhinz@unr.edu](mailto:nhinz@unr.edu), [jnatukunda@gmail.com](mailto:jnatukunda@gmail.com), [emisabirye@gmail.com](mailto:emisabirye@gmail.com),  
[wcumming@wcumming.com](mailto:wcumming@wcumming.com)

### **Keywords**

*Geological structures, geophysical data, hydrothermal fluids, basin and ranges region.*

## ABSTRACT

Panyimur geothermal prospect is located near the northern end of the Lake Albert Basin within the western branch of the East African Rift System. It has several hot springs, the maximum surface temperature of all them is 61.4°C. Other surface manifestations are: active and inactive travertine deposits and inactive amorphous silica deposits.

Substantial surface exploration has been conducted at this prospect, including regional geological mapping (1961), geological investigations in 2011 and 2012, a gravity survey in 2011-2012, a follow up gravity and ground magnetics study 2015, MT/TEM data in 2016 acquisitions and additional MT in 2017 as well as petroleum exploration wells, 2D seismic profiles.

In this study, fault traces were mapped in detail to refine the conceptual model for this prospect, which has been characterized as a likely fault-related geothermal system. The fluid flow pathways in such systems are typically controlled by normal fault step overs, fault terminations, and major fault intersections. The recency of rupture was also evaluated for each major fault segment. Exposed fault surfaces were analyzed to determine the dip of the faults, the sense of motion along these faults and the local stress field. These surficial data has been combined with existing and new acquired MT/TEM, seismic geophysical studies in the past several years to update the conceptual model for this geothermal prospect.

The Panyimur geothermal area appears to be a fault-controlled system that is associated with a 1.5 to 2 km-wide step-over linking two NNE-striking faults. The local and regional geomechanical data indicate that these NNE-striking faults are nearly pure dip-slip, making this setting a step-over between pure normal faults in contrast to a pull-apart between oblique- or strike-slip faults. Normal fault step-overs are the most common structural setting for geothermal systems in the Basin and Range region in the United States. Two models have been derived; a fault-hosted resource model and a sedimentary resource option with two isothermal patterns on a MT resistivity cross-section. Both models, which have been used to target Temperature Gradient Holes (TGHs), assume that the resource is fault-hosted (with no direct magmatic contribution of heat or fluid) and heated by deep circulation to 3000 or 4000m depth.

## 1. Introduction

Panyimur is one of the most prospective geothermal areas in Uganda. Although substantial surface exploration has been conducted at this site, this prospect is not well-understood. Following up recommendations in 2017 from earlier geophysics studies and many years of earlier geoscience studies, there is a need to review the existing data and conduct additional geological, geophysical and geochemical work at this prospects in order to allow development of more robust conceptual models that can be used to target shallow TGH. This paper discusses the structural mapping component that was conducted in September 2017, and which was accomplished by a team of staff associated with the Ugandan Geothermal Resources Department (GRD) of the Ministry of Energy and Mineral Development (MEMD), who worked closely with East African Geothermal Energy Facility (EAGER) consultants.

### 1.1 Location and Accessibility

The Panyimur geothermal area is located near the north end of the Lake Albert basin (Fig. 1). It is located on topographic map sheet 29/2 (Pakwach) in the administrative district of Nebbi in the old region of Southern West Nile, at the mouth of the Albert Nile, as it leaves Lake Albert (Fig. 1) and standing opposite the northern edge of the delta of the Victoria Nile.

The area can be accessed by the Kampala – Karuma – Pakwach – Nebbi tarmac road for a distance of 426 km to Nebbi town. At Nyaravur Trading Centre, 16 km before Nebbi, and the famous trading outpost for the ‘grinding stone’ of Angal, a south-running murram road leads to Parombo town via Angal Roman Catholic Mission and Trading Centre. This area has hot springs that are presently undeveloped apart from the onsite bathing and laundry by local villagers.

### 1.2 Objective of the study

The specific goals included providing greater detail of the late Cenozoic fault characteristics, defining the location and nature of the active and inactive surficial geothermal manifestations, and characterizing formations that might promote fracture permeability or host sufficient formation permeability to host a geothermal reservoir.

### 1.3 Methodology

Fault traces were mapped in detail to refine the conceptual models for the Panyimur geothermal prospect area, which have been characterized in the earlier similar studies as likely fault-related geothermal systems. The fluid flow pathways in such systems are typically controlled by normal fault step overs, fault terminations, and major fault intersections (e.g., Hinz et al., 2014; Faulds and Hinz, 2015). The recency of rupture (Quaternary versus pre-Quaternary) was also evaluated for each major fault segment. Exposed fault surfaces were analyzed to determine the dip of the faults, the sense of motion along these faults (e.g., normal slip versus strike-slip), and the local stress field. These surficial data are being combined with existing geophysics and geochemistry data to update conceptual models for this geothermal area.

## 2. Geological setting of Panyimur area

The Lake Albert basin (Fig. 1) is an approximately 200 km-long, NE-trending, NW-tilted half-graben in the northern part of the Albertine Rift of the western branch of the East African Rift System (EARS). This basin reaches 5 km deep and is filled with syntectonic, Miocene to present-age lacustrine and fluvial sediments that are deposited on Precambrian metamorphic basement. Lake Albert itself is more than 150 km-long and locally over 40 km-wide (Fig. 1). Due to its rapid sedimentation, it is relatively shallow with water <35 m-deep. In contrast to the eastern branch of the EARS, particularly the Gregory Rift segment in Kenya, the Albertine Rift geothermal prospects appear to be amagmatic. In particular, the Lake Albert segment of the Albertine rift (Fig. 1) is not associated with any known recent volcanic centres. Extension in the Albertine Rift area began in the middle to late Miocene (Ebinger, 1989; Cohen et al., 1993) and is active today (e.g., Midzi, et al., 1999).



**Figure 1: Panyimur, Buranga and Kibiro geothermal prospects in Western Uganda. Hachured block corresponds to approximate boundary of western branch of the EARS.**

Similar to the Gregory Rift in the eastern branch of the EARS, the extension direction may also have changed since the middle Miocene from NE-SW to NW-SE (e.g., Strecker et al., 1990). Resolved earthquake focal mechanisms from the Lake Albert basin show a nearly pure extensional environment with average  $S_{\min}$  oriented WNW-ESE (Heidbach et al., 2007; Delvaux and Barth, 2010). GPS geodetic strain measurements and block models also indicate WNW-ESE-oriented motion across the Albertine Rift (Calais et al., 2006; Saria et al., 2014; Stamps et al., 2008; 2014).

## 2.1 Previous Studies

Hepworth (1961) conducted regional geologic mapping focusing on late Cenozoic geomorphology of the Nile in and around the northern part of the Lake Albert basin. Hepworth's maps show the major strands of the Lake Albert basin faults and the distribution of late Cenozoic fluvial and lacustrine deposits that record the interplay between basin formation, and incision by the Nile River system. GRD conducted geologic investigations during 2011 and 2012 in the Panyimur area, including measuring foliation and fracture orientations in the banded gneiss, and mapping the regional distribution of late Cenozoic diatomite in lacustrine deposits (GRD, 2012; Kato, 2013). GRD also conducted a series of geophysical studies in the past several years, including a gravity survey in 2011-2012, a follow up gravity and ground magnetics study 2015, and acquisition of MT/TEM data in 2016 and additional MT in 2017 and 2018. Relevant data is also available from petroleum exploration wells (e.g., Ondyek-1 drilled in 2013), 2D seismic profiles, and village water wells.

### 2.1.1 Stratigraphic Framework

The stratigraphic framework consists of two dominant units, Precambrian metamorphic basement, and late Cenozoic basin-fill deposits. The Precambrian basement is dominated by flaggy gneiss with some banded paragneiss, felsic paragneiss, and amphibolite (Harma et al., 2011; GRD, 2012; this study). The foliation in the basement rocks strikes consistently NNW to NW and dips consistently ENE to NE (Fig. 2). Most of the foliation is bedding parallel in the paragneiss. The Cenozoic basin-fill consist of syntectonic lacustrine and fluvial-lacustrine sediments composed of intercalated silt, sand, and gravel. These basin-fill deposits approach 5 km-thick in the Lake Albert basin (EARGER, 2017). Located 3.5 km SSW of Panyimur hot springs, the Ondyek-1 well penetrates about 1350 m (TVD) of basin fill without intersecting the basement. Based on gravity models, the depth of basin fill in the Panyimur area probably does not exceed ~1.5 km (EARGER 2017). In the vicinity of Panyimur, seismic reflection profiles indicate that these sediments dip gently WSW, obliquely into the basin-bounding fault, so buoyant thermal flow diverted from a fault-hosted upflow into a formation-hosted aquifer would outflow to the ENE, beneath the lake. Locally, fluvial or fluvial-lacustrine gravels mantle the exposed gneiss between the two major faults, reaching a maximum of 2 m thick, but are mostly <1 m thick and are not mapped as a separate unit in this area.

## 3.0 DATA PRESENTATION, ANALYSIS AND INTERPRETATION

### 3.1 Structural Framework and Geomechanics

The Panyimur area is dominated by two major NNE-striking faults with normal, down-to-east displacement, and are known in this report as the Upper fault and the Lower fault (Fig. 2). The Upper fault offsets only Precambrian metamorphic rocks with a 75 to 95 m scarp, whereas the Lower fault, located from 600 to 2000 m to the southeast of the Upper fault, offsets the Precambrian by perhaps 1500 m, although its scarp is smaller at 40-70 m high, due to infill by sediments. There is also a secondary set of minor NE- to ENE-striking, north and south dipping faults with dextral-normal or sinistral-normal sense of displacement. The two major NNE-striking bounding faults are locally linked through a left fault step, 1-2 km southwest of Panyimur hot springs. The major NNE-striking faults also make left steps on the scale of 100 m to 600 m, with some local right step on the scale of 100 m to 200 m (Fig. 3). Based on fault surface measurements in the field, the Lower fault dips 43° to 50° ESE (Fig. 4) and the Upper fault dips 60° to 65° ESE. The moderate dip on the Lower fault is consistent with dips inferred by earlier EAGER studies from seismic reflection data and MT profiles.

The NE and ENE-striking oblique-slip and strike-slip faults range in dip from 55° to 90° (Fig. 5). Quaternary fault scarps are associated with both the Upper and Lower faults and also with part of the sinuous fault in the step-over that links the two major faults (Fig. 2). A fault scarp in Quaternary basin fill deposits is associated with one of the NE-striking faults located about 6 km SSW of the hot springs (south off the boundary of Fig. 2). Aside from this one NE-striking fault, Quaternary fault scarps were not observed along the other NE- and ENE-striking faults.

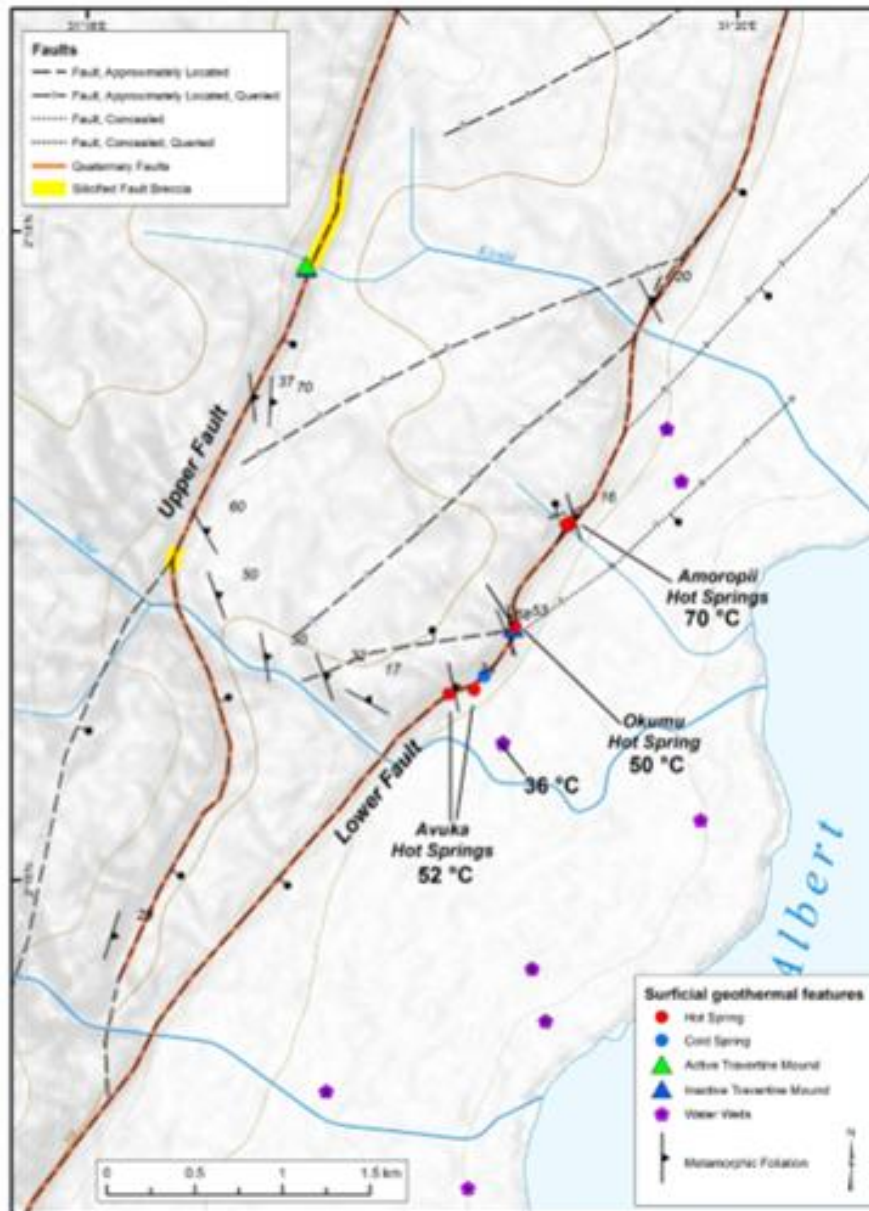


**Figure 2:** Structural geology map of the Panyimur geothermal area with active and inactive surficial geothermal features. Temperature data of wells and springs are maximum measured temperatures for each area.



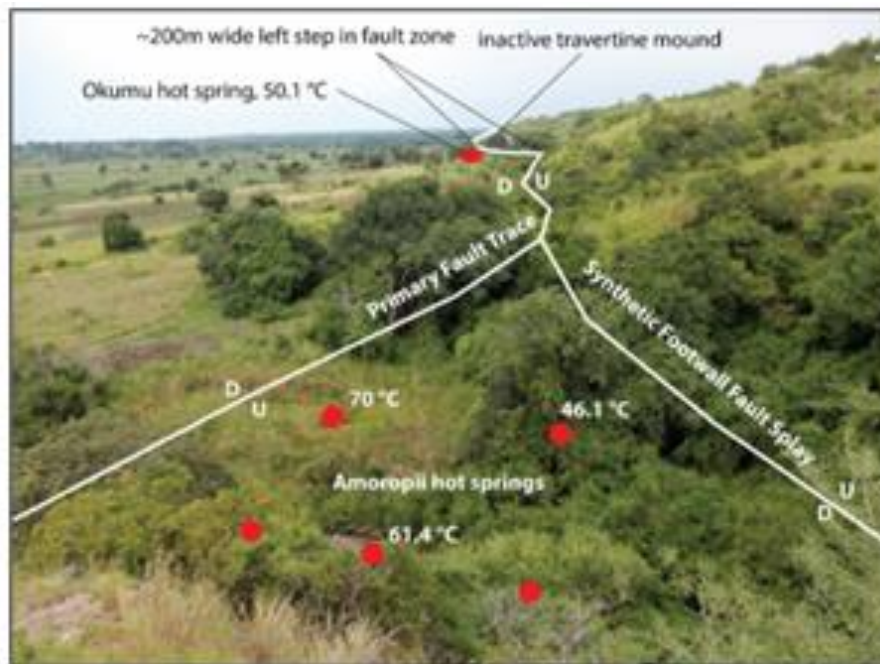


**Figure 3.** View looking SSW along the Lower fault with hot springs associated with steps in the fault system (Fig. 2). Red dots correspond to hot key springs locations within this field of view. Not all hot springs associated with Amoropii are shown.



**Figure 4.** MEMD staff Edward Isabirye, James Natukunda, and Isa Lugayizi, collecting structural data on a fault surface associated with the Lower fault, locally dipping 43° E.



**Figure 5.** MEMD staff Edward Isabirye and James Natukunda collecting structural data along an ENEstriking fault in the footwall of the Lower NNE-striking normal fault, ~30 m north of Amoropii hot springs.

Twelve kinematic measurements were obtained from nine fault surfaces exposed in the Panyimur geothermal area (Figs. 4, 5, 6A1). Analysis of all these data indicate that faulting in this area has evolved under at least two stress regimes (Fig. 6A). Given the assumption that the strain is linearly related to stress (e.g., Sippel et al., 2009), the results of analysis of the group of NNE-striking faults (Fig. 6B1, 6B2) are  $P = \sigma_1 = 108^\circ/70^\circ$ ;  $B = \sigma_2 = 031^\circ/17^\circ$ ;  $T = \sigma_3 = 297^\circ/10^\circ$  (trend/plunge) with  $Shmin = N63^\circ E$ . The results of analysis of the NE- to ENE-striking faults (Figs. 6C1, 6C2) are  $P = \sigma_1 = 247^\circ/26^\circ$ ;  $B = \sigma_2 = 106^\circ/66^\circ$ ;  $T = \sigma_3 = 340^\circ/11^\circ$  (trend/plunge); with  $Shmin = N20^\circ W$ . Figures 6A3, 6B3, 6E3 are fluctuation histograms of the dihedral angle between the measured lineation and the stress vector (the resolved shear stress direction) for each fault plane. Generally populations with less than  $15^\circ$  or  $20^\circ$  fluctuation between the measured lineation and the resolved shear stress direction correspond to a uniform stress field. These fault data indicate two stress regimes, one as a normal faulting regime with  $\sigma_1$  oriented vertically and  $Shmin$  oriented  $N63^\circ W$ , the second as a strike-slip faulting regime with  $\sigma_2$  oriented vertically and  $Shmin$  oriented  $N20^\circ W$  (Fig. 6). It is probable that one stress regime is a paleo-stress analogous to the change in extension direction in Great Basin region of the USA from WSW-ENE in the Miocene to WNW-ESE in the present, or the Kenya Rift where the extension direction has changed from SW-NE in the early Miocene to NW-SE in the present (Strecker et al., 1990). It is possible that early faulting associated with the Albertine rift initiated on NE- to ENE-striking strike-slip and oblique slip faults and then transitioned to largely pure dip-slip motion on the NNE-striking basin-bounding faults that are active today.



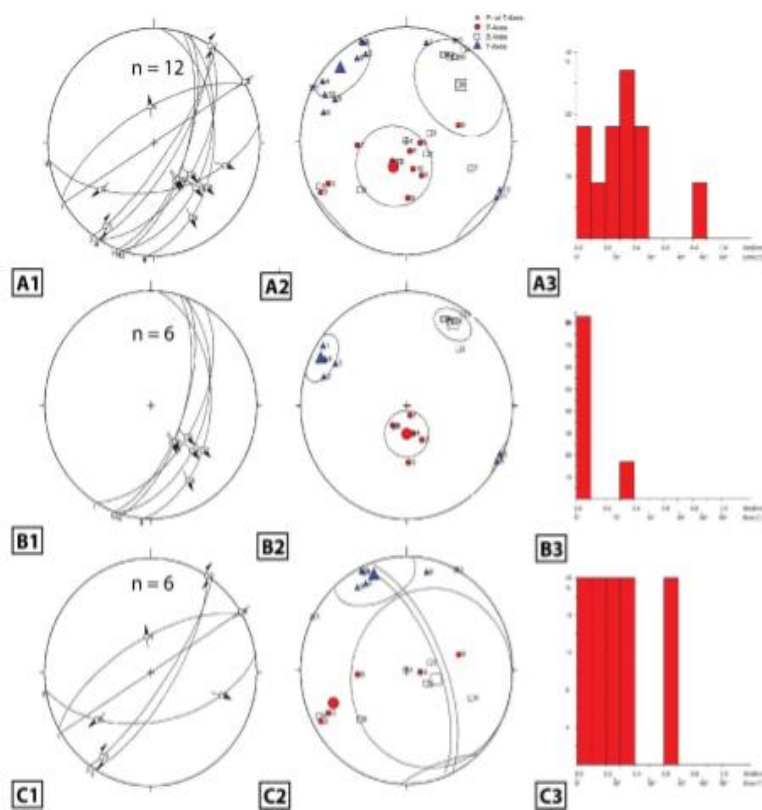


**Figure 6.** Fault kinematic data and stress inversion calculations. (A) All kinematic data collected in 2017. (B) Kinematic fault data for the NNE-striking normal faults. (C) Kinematic data for NE- to ENE-striking faults (Source: EARGER Report U 23/D 02).

(A1, B1, C1) Lower hemisphere stereographic projection of great circles of exposed faults,  $n$  = number of data points. Arrows indicate slip directions inferred from striations and other kinematic indicators (e.g., Riedel shears). (A2, B2, C2) P/T axis diagrams, showing the orientations of principal strain axes for each measured fault. Large symbols are mean vectors to all P, B and T axes and represent the strain field. All analyses conducted with Tectonics FP using numeric dynamic analysis and a theta angle of  $30^\circ$ .

### 3.2 Surficial Geothermal Features

Hot springs are distributed in three clusters along a 1.25 km-long segment of the Lower fault (Figs. 2, 3). The three hot spring clusters go by local names, from north to south these are Amoropii, Okumu, and Avuka. The Amoropii hot springs emanate in the active stream bed and in a swampy area directly south of the unnamed stream. The highest temperature spring in the stream bed was measured at  $61.4^\circ\text{C}$  in 2017. GRD previously recorded a temperature of  $70^\circ\text{C}$  in a spring in the swampy area south of the stream. However this pool was not accessed during this 2017 trip because thick vegetation made access unsafe. Okumu hot spring was measured  $50.1^\circ\text{C}$  in 2017 and is located below an inactive travertine mound. A maximum temperature of  $52^\circ\text{C}$  was recorded at the Avuka hot springs, however there are more springs within an area of heavily vegetated swampy ground that were inaccessible for measurement in 2017. A village water well with a hand pump located about 400m SE of the hot springs produces  $36^\circ\text{C}$  fluids.

Inactive travertine spring mounds are associated with both the Upper and Lower faults (Figs. 2, 7, 8). Active travertine mounds are only building along the Upper fault (Fig. 9). Fault

breccia is locally cemented with amorphous silica and quartz druse along the Upper fault, adjacent to Kivuje stream (Figs. 2, 10). No active silica deposition was observed across this geothermal area.



**Figure 7.** Inactive travertine mound above Okumu hot spring along the Lower fault (Fig. 2).



**Figure 8.** Inactive travertine mound (travertine in upper right of photo) undercut by the Kivuje stream, along the Upper fault (Fig. 2).





**Figure 9.** Active travertine deposition associated with cold springs along Kivuje stream along the Upper fault (Fig. 2).



**Figure 10.** Quartz druse and amorphous silica veins in fault breccia damage zone in Precambrian gneissic basement along the Upper fault (Fig. 2).

### 3.3 Structural Model for Panyimur

The Panyimur geothermal area is associated with a 1.5 to 2 km-wide step-over linking two NNE-striking faults. The local and regional geomechanical data indicate that these NNE-striking faults are nearly pure dip-slip, making this setting a step-over between pure normal faults in contrast to a pull-apart between oblique- or strike-slip faults. Normal fault step-

overs are the most common structural setting for geothermal systems in the Basin and Range region of the USA (Faulds and Hinz, 2015). Producing geothermal systems associated with normal fault step-overs include Desert Peak (Nevada), Bradys (Nevada), Jersey Valley (Nevada), McGinness Hills (Nevada), and Neal Hot Springs (Oregon). In many of these areas, surficial geothermal manifestations are focused locally along small scale fault steps within the larger fault step-over (e.g., Bradys). The hot springs at Panyimur are also coincident with small fault steps along the lower NNE-striking fault within the larger step-over region.

Based on the distribution of active hot springs, the primary locus of upflow is probably along the Lower fault with fluid flow locally focused up and down dip within the small-scale steps along this fault. The silica veins in the fault breccia of the Upper fault indicate probable past geothermal upflow along that fault. However, it is unknown whether the Upper fault still hosts hydrothermal circulation at depth. The cool water springs along the upper fault could involve cold water circulating at shallow depths and/or involve cool downflow infiltrating to potential geothermal reservoir depths. Faults that bridge the step-over and strike oblique to the primary NNE-striking faults could also facilitate concealed hydrothermal fluid flow with no surface thermal manifestations. Thus, future exploration plans should consider one conceptual model that includes some hydrothermal fluid flow within the step-over between the two large NNE-striking faults rather than only associated with the Lower fault.

Potential reservoir models at Panyimur include: 1) fault/fracture hosted permeability within the damage zone and fault splays directly associated with the Lower fault; 2) outflow into basin-fill sediments from this fault; 3) combination of scenarios 1 and 2; and 4) scenario 1 connected to flow through part of the step over region between the two major NNE-striking faults.

#### **4.0 DISCUSSION, CONCLUSIONS & RECOMMENDATIONS FOR FUTURE WORK.**

The structural mapping and geophysical in this study has improved, together with the geochemical interpretations, the structure model for Panyimur. The data analysis and interpretation confirm the prospects is a heated by deep fluid circulation in structures and have resource temperatures in a range of 110-150°C, similar to several developed geothermal fields in the Basin and Range geothermal region of the United States.

It is recommended that additional spring and water well temperature data be collected in the two water wells 700 to 800 m NE of the Amoropii hot springs cluster. Temperatures should be measured from other area water wells to map out the overall pattern of elevated shallow temperature in this part of the basin. Additionally, temperature measurements for all springs at Avuka hot springs cluster ought to be completely measured to see if any vents might be hotter than the one in which a maximum temperature of 52°C was previously measured.

Based on data available for MT and TEM geophysical surveys, recommendations are to drill up to eight temperature gradient wells. One strategy would be to position six TGHs located about 300 m east of the Lower fault, in a line parallel to the fault at about 1 km spacing to capture the 6 km strike-length of the primary step-over. Two holes positioned between the upper and lower faults, WNW of the hot springs to will be useful to determine if the reservoir extends between the two faults or is confined to the lower fault zone.

It is also possible that the MT-TEM models and/or the initial TGH results could lead to drilling one or more alternative locations farther from the fault in order to investigate potential outflow into the basin. The holes along the lower fault should be started adjacent to the hot springs and then extended north and south until the edge of the thermal anomaly is reached in each direction. Thus it is possible that an entire line of six TGHs may not be needed if the thermal anomaly does not extend the full length of the step-over.

In combination with drilling temperature gradient holes, it is recommended to conduct additional detailed fault mapping along the lower fault to: 1) capture greater detail of the numerous steps and fault bends along the fault trace, 2) map additional footwall and hanging wall fault splays, and 3) map the ENE- to NE striking faults that intersect the lower fault in greater detail.

Together, the additional structural geology data in combination with additional temperature data will facilitate developing updated conceptual models in greater detail and reduce the risks involved in targeting deeper slim holes during subsequent exploration.

### **Acknowledgement**

Isa Lugaizi would like to thank the following persons: In Uganda: the staff of Geothermal Resources Department, especially Mr. Godfrey Bahati, Mr. Vicent Kato, Mr. Edward Isabirye, Mr. James Francis Natukunda and Mr. Peter Mawejje for their support and fruitful discussion during and after the field investigation.

The East Africa Geothermal Facility (EARGER), especially Mr. Nicholas Hinz and William (Bill) Cumming for the mentoring during field collection, carefully reading through this manuscript and for permission to use the information and data in this paper.



## REFERENCES

- Calais, E., Ebinger, C., Hartnady, C., and Nocquet, J.M., “Kinematics of the East African Rift from GPS and earthquake slip vector data”: In, Yirgu, G., Ebinger, C. J. and Maguire P. K. H., eds., “The Afar volcanic province within the east African Rift System”: Geological Society Special Publication, London, United Kingdom, v. 259, (2006), p. 9–22.
- Cohen, A., M. Soreghan, and C. Scholz., “Estimating the age of formation of lakes: An example from Lake Tanganyika, East African rift system”: *Geology*, v. 21, (1993), p. 511–514.
- Delvaux, D., and Barth, A., “African stress pattern from formal inversion of focal mechanism data”: *Tectonophysics*, no. 482, (2010), p. 105-128.
- Ebinger, C. J., “Tectonic development of the western branch of the East African rift system”: *Geological Society of America Bulletin*, v. 101, (1989), p. 952–967.
- EAGER, “Structural geology at Panyimur and Buranga” (2017) Final Report No. U23/D 02.
- Faulds, N.H., and Hinz, N.H., “Favorable tectonic and structural settings of geothermal settings in the Great Basin Region, western USA: Proxies for discovering blind geothermal systems”: *Proceedings, World Geothermal Congress, Melbourne, Australia*, (2015), 6 p.
- GRD, “Progress report on geological investigations of Panyimur geothermal resource area, Nebbi District” (2012), 21 p.
- Härmä, P., de Kock., G., Koistinen, T., Manninen, T., Mäkitie, H., Pokki, J., Westerhof, P., Pekkala, Y., Kuivasaari, T., Kärkkäinen, N., Konnunaho, J., 2011, “PAKWACH Sheet” Number NA-36-5, scale 1:250,000, (2011).
- Heidbach, O., Tingay, M., Barth, A., Reinecker, J., Kurfe, D. and Müller, B., “The World Stress Map database release” (2008).
- Hepworth, J.V., “Geological map of Paihda”: Sheet 28 and 29 (NA-36 G-IV and H-III), scale 1:100,000, (1961).
- Hinz, N.H., Faulds, J.E., and Coolbaugh, M.F., “Association of fault terminations with fluid flow in the Salt Wells geothermal field, Nevada, USA”: *Geothermal Resources Council Transactions*, v. 38, (2014), p. 3-9.
- Kato, V., “Geothermal exploration in Uganda status report: Short Course VIII on Exploration for Geothermal Resources, UNU-GTP, GDC, KenGen, at Lake Bogaria and Lake Naivasha, Kenya” (2013), 27 p.
- Midzi, V., Hlatywayo, D.J., Chapola, L.S., Kebede, F., Atakan, K., Lombe, D.K., Turyomurugyendo, G. and Tugume, F.A., “Seismic hazard assessment in Eastern and Southern Africa”. *Annali di Geofisica*, v. 42, no. 6, (1999), p. 1067-1083.
- Saria, E., Calais, E., Stamps, D.S., Delvaux, D., and Hartnady, C.J.H., “Present-day kinematics of the East African rift: *Journal of Geophysical Research*”: *Solid Earth*, v. 119, (2014), p. 3584-5600.
- Sippel, J., Scheck-Wenderoth, M., Reicherter, K., and Mazur, S., “Paleostress states at the southwestern margin of the Central European Basin System — Application of fault-slip analysis to unravel a polyphase deformation pattern”: *Tectonophysics*, no. 470, (2009), p. 129-146.

- Stamps, D.S., Calais, E., Saria, E., Hartnady, C., Nocquet, J-M, Ebinger, C.J., and Fernandes, R.M. “A kinematic model for the East African Rift: Geophysical research letters (2008), 6 p.
- Stamps, D.S., Flesch, L.M., and Ghosh, A. “Current kinematics and dynamics of Africa and the East African rift system”: *Journal of Geophysical Research: Solid Earth*, v. 119, (2014), p. 5161-5186.
- Strecker, M.R., Blisniuk, P.M., and Eisbacher, G.H. “Rotation of extension direction in the central Kenya Rift”: *Geology*, v. 18 (1990), p. 299-302.